The Role of Diffusivity Changes on the Pattern of Warming in Energy Balance Models

CHIUNG-YIN CHANG[a] AND TIMOTHY M. MERLIS[a]

[a] *Program in Atmospheric and Oceanic Sciences, Princeton University, Princeton, New Jersey*

(Manuscript received 3 March 2023, in final form 30 June 2023, accepted 16 August 2023)

ABSTRACT: Atmospheric macroturbulence transports energy down the equator-to-pole gradient. This is represented by diffusion in energy balance models (EBMs), and EBMs have proven valuable for understanding and quantifying the pattern of surface temperature change. They typically assume climate-state-independent diffusivity, chosen to well represent the current climate, and find that this is sufficient to emulate warming response in general circulation models (GCMs). Meanwhile, model diagnoses of GCM simulations have shown that the diffusivity changes with climate. There is also ongoing development for diffusivity theories based on atmospheric dynamics. Here, we examine the role that changes in diffusivity play in the large-scale equator-to-pole contrast in surface warming in EBMs, building on previous analytic EBM theories for polar-amplified warming. New analytic theories for two formulations of climate-state-dependent diffusivity capture the results of numerical EBM solutions. For reasonable choices of parameter values, the success of the new analytic theories reveals why the change of diffusivity is limited in response to radiative forcing and does not eliminate polar-amplified warming.

KEYWORDS: Atmospheric circulation; Eddies; Energy transport; Climate change

1. Introduction

Atmospheric macroturbulence plays a leading-order role in determining the meridional distribution of temperature. A simple conceptual picture is to consider this large-scale turbulence as acting to transport energy down the equator-to-pole energy gradient, a downgradient diffusion (Held 1999). One application of the diffusive picture is to use it as a turbulence closure and avoid explicitly simulating atmospheric motions in energy balance models (EBMs). Here, the radiative fluxes are typically assumed linear functions of surface temperature for simplicity, and the atmospheric energy transport is governed by the gradient of surface temperature (dry EBMs) or surface moist static energy (moist EBMs).

Recently, moist EBMs have been used to emulate the temperature change pattern of comprehensive climate models with prescribed radiative feedback parameters and surface fluxes to the ocean (e.g., Hwang and Frierson 2010; Hwang et al. 2011; Bonan et al. 2018; Armour et al. 2019; Russotto and Biasutti 2020; Beer and Eisenman 2022; Hill et al. 2022). There has also been theoretical understanding of these EBMs (Flannery 1984; Merlis and Henry 2018) for radiatively forced climate change, highlighting the role that additional latent energy transport with warming can play in polar amplification. While much of EBM research has focused on the role of the spatial pattern of radiative feedbacks or the role of moisture in energy transport changes, there has been relatively limited analysis of cases with climate-state-dependent diffusivity and the role of diffusivity changes on the pattern of warming.

Most EBM research that seeks to emulate the behavior of general circulation model (GCM) simulations has neglected potential changes of diffusivity (e.g., Hwang and Frierson 2010; Bonan et al. 2018; Armour et al. 2019), even though diffusivities are known to change in the GCM rung of models. Aquaplanet atmospheric GCM simulations simulate decreases in the midlatitude diffusivities in response to uniform surface warming (Fig. 2a of Shaw and Voigt 2016), but the midlatitude maximum may increase (Fig. 4a of Mooring and Shaw 2020). Lu et al. (2022) also found a general reduction in midlatitude diffusivities in GCM simulations of the response to increased CO_2 concentration that allow for meridional temperature gradients to weaken (their Fig. 3). Finally, the coupled model simulations analyzed by Wu et al. (2011) show increases in diffusivity in both hemispheres in a DJF average of a transient warming scenario (their Figs. 6c–e). We also note that diffusive theories developed for GCM simulations of climate change do require climate-state-dependent formulations to capture the behavior over a wide range of climates (e.g., Frierson et al. 2007; Bischoff and Schneider 2014; Liu et al. 2017; Merlis et al. 2022; Lu et al. 2022).

Existing theories for the diffusivity $\mathcal{D}$ have indeed suggested a variety of climate-state-dependent formulations, but there remains a lack of agreement on a form that nicely describes the behavior of Earth's atmosphere. The starting point for these theories may be based on (quasi-)linear baroclinic instability theory (e.g., Green 1970; Stone 1972; Schneider 2006) or fully developed quasigeostrophic turbulence theory (e.g., Held and Larichev 1996; Barry et al. 2002; Chang and Held 2022), but their common goal is to seek for a closure that expresses the diffusivity as a function of external forcing and planetary parameters or, at least, the environmental mean-state

Denotes content that is immediately available upon publication as open access.

Corresponding author: Chiung-Yin Chang, cychang@princeton.edu

DOI: 10.1175/JCLI-D-23-0121.1

variables. Given the baroclinic nature of atmospheric macroturbulence, these variables are naturally the vertical wind shear and deformation radius, or equivalently temperature gradient $\partial_y T$ and static stability $\partial_z T$, in dry atmospheres. Since typical EBMs do not contain a vertical dimension, it is then the quantitative dependence of the diffusivity on the meridional temperature gradient [e.g., the power-law dependence of $\mathcal{D} \propto (\partial_y T)^k$] that varies among the different theories, with the concomitant assumptions about the relationship between vertical and horizontal fields. Efforts to extend the dry theories and further consider the role of water vapor is however difficult, as the presence of moisture and the associated latent energy release may fundamentally alter the underlying dynamics (e.g., Frierson et al. 2007; O'Gorman and Schneider 2008). From a global entropy budget perspective, Chang and Held (2022) hypothesized that, so long as it is the diffusion of moist enthalpy of interest, the corresponding diffusivity would likely depend on moist enthalpy gradient as well. In the context of moist EBM theory, this suggests that the diffusivity may depend on the moist static energy (MSE) gradient in addition to the temperature gradient.

It is therefore interesting to ask how the warming pattern in moist EBMs—polar amplification in particular—is affected if the diffusivity is allowed to vary with climate states. Addressing this question is valuable in that it helps bound the errors associated with neglecting climate-state-dependent diffusivity, as this is the little-scrutinized standard practice in the previous work.

Here, we build on the analytic moist EBM theory developed by Merlis and Henry (2018, hereafter MH18) to offer new analytic progress on understanding how changing diffusivity impacts the pattern of warming. Motivated by the diffusivity dependencies identified in previous GCM simulations and proposed by existing scaling theories, we consider two climate-state-dependent forms of diffusivity. The first depends linearly on global-mean temperature and the second scales with the temperature and MSE gradients with some power-law dependence. In what follows, we present the EBM formulation and review the theoretical results of MH18 in section 2, analyze the results for a global-mean temperature-dependent diffusivity in section 3 and the results for temperature- and MSE-gradient-dependent diffusivities in section 4, both with a comparison between theoretical estimates and numerical simulations of EBM solutions. We then discuss the relationships of our results and previous studies in section 5 and offer conclusions in section 6. A nondimensional form of the theory is included in the appendix.

2. Energy balance models

a. Governing equation

The diffusive EBM is governed by a one-dimensional partial differential equation

$$C\partial_t T(x) = \frac{1}{4} QS(x)a(x) - [A + BT(x)] - \nabla \cdot \mathbf{F}_a(x) + \mathcal{F}, \quad (1)$$

with heat capacity C, surface temperature $T(x)$, $x = \sin\phi$ with latitude ϕ, solar constant Q, insolation structure function $S(x)$, co-albedo $a(x)$, outgoing longwave radiation OLR $= A + BT(x)$, atmospheric energy flux divergence $\nabla \cdot \mathbf{F}_a(x)$, and radiative forcing $\mathcal{F}$. Given that we are interested in equilibrium solutions, our analysis is focused on $\partial_t T(x) = 0$, and we compare them to numerical steady states obtained via time-marching of the above equation, with details of numerical methods as described in MH18.

Here, we are focused on the role of climate-dependent diffusivity, so we keep the radiation simple and identical to MH18. For the shortwave, the insolation is time independent and similar to Earth's annual mean: $Q = 1360$ W m^{-2} and $S(x) = 1 - S_2 P_2(x)$, with $S_2 = 0.482$ and $P_2(x) = (3x^2 - 1)/2$ the second Legendre polynomial. The co-albedo is a climate-state-independent function that captures the structure of Earth's annual-mean planetary albedo: $a(x) = a_0 + a_2 P_2(x)$ with $a_0 = 0.68$ and $a_2 = -0.2$. Both are as in North et al. (1981). For the longwave, both components of the OLR have constant parameter values of $A = 281.67$ W m^{-2} and the longwave feedback parameter that is spatially uniform with a value of $B = 1.8$ W m^{-2} K^{-1}. The radiative forcing that we use is spatially uniform with a value $\mathcal{F} = 3.6$ W m^{-2}, inspired by the global-mean radiative forcing of a doubling of CO_2. We emphasize that we are not prescribing spatially varying forcing, feedbacks, or ocean heat uptake to emulate comprehensive GCMs (e.g., Hwang and Frierson 2010; Hwang et al. 2011; Bonan et al. 2018; Armour et al. 2019; Russotto and Biasutti 2020; Beer and Eisenman 2022; Hill et al. 2022). The interactions of radiation with clouds, sea ice, and seasonal cycle have been shown to strongly affect the magnitude of polar amplification (e.g., Kim et al. 2018; Feldl and Merlis 2021) and give rise to intermodel spread among comprehensive GCMs (e.g., Hwang et al. 2011; Bonan et al. 2018). Given their uncertainties, we leave them out in our EBM so that we can more cleanly isolate the role of diffusivity changes, while acknowledging that a complete EBM theory would include spatially varying radiative feedbacks and forcing.

The divergence of the atmospheric energy flux is governed by diffusion of MSE: $\nabla \cdot \mathbf{F}_a(x) = -\partial_x[\mathcal{D}(1 - x^2)\partial_x h(x)]$, with diffusivity $\mathcal{D}$ and surface MSE defined in units of temperature $h(x) = T(x) + L\mathcal{H}c_p^{-1}q^*[T(x)]$. The latent heat of vaporization $L = 2.5 \times 10^6$ J kg^{-1} and the heat capacity of air at constant pressure $c_p = 1004.6$ J kg^{-1} K^{-1} are both constant. The relative humidity $\mathcal{H}$ is spatially constant with a standard value of 0.8. Setting $\mathcal{H}$ to zero converts the moist EBM to a dry EBM.

To keep the analysis straightforward, we consider variants of the EBM with a spatially constant $\mathcal{D}$. The climate-state dependence is introduced by varying its value either as scaled by the global-mean temperature or as simple functions of the equator-to-pole temperature and/or MSE contrast evaluated as the coefficients of Legendre polynomials. Legendre polynomials, $P_i(x)$ with the order of the Legendre polynomials indicated by subscripts, are a set of orthogonal basis functions for the sphere and a series solution to the EBM governing equation has been widely used (e.g., North 1975). As will be discussed in the next section, we follow MH18 to derive analytic estimates for the EBM solutions considering an approximation truncated at the second Legendre polynomial. Therefore, the two Legendre polynomials of interest here are the zeroth and

second order. By definition, the zeroth order corresponds to the global mean, so T_0 measures the global mean temperature. We use the second-order Legendre polynomial components as the relevant metric for large-scale gradients, so T_2 measures the equator-to-pole temperature contrast and will be used to describe temperature change patterns, such as whether they are polar amplified or not.

In addition to a climate-invariant diffusivity $\mathcal{D} = \overline{\mathcal{D}}$ [throughout, $\overline{(\cdot)}$ indicates a control climate value], we introduce the first category climate-state-dependent diffusivity with the form

$$\mathcal{D}(T_0) = \overline{\mathcal{D}}[1 + \gamma(T_0 - \overline{T}_0)], \tag{2}$$

where the temperature sensitivity of the diffusivity γ for a global-mean temperature change can be expressed in % K^{-1} for comparison to that of the Clausius–Clapeyron (CC) relation. One can motivate the $\mathcal{D}(T_0)$ analysis from an uncertainty quantification perspective: a standard moist EBM formulation has a spatially constant and climate invariant diffusivity. Our aim is to evaluate the neglect of climate-state-dependent diffusivity on the pattern of warming. The logical starting point for this quantification is to examine the sensitivity of a diffusivity that varies in proportion to the global-mean temperature $\mathcal{D}(T_0)$. One can think of this as encapsulating the net effect of other aspects of the climate statistics that may more directly determine the diffusivity $\mathcal{D}$. So, we extend the analytic theory and numerical calculations of moist EBM to this case.

The other category of climate-state-dependent diffusivity that we consider responds to gradients. As discussed in the introduction, given the lack of consensus on the particular power law that quantitatively captures the dependence of the diffusivity on the meridional temperature or MSE contrast, we provide a theory for the general case. The state variable of the EBM is surface temperature T and the derived quantity surface MSE h is, of course, readily available. As there is no vertical information available, we must assume that the diffusivity is proportional to these surface quantities that are available and then modify the exponent. In other words, we assume there is a relationship between the vertically varying information (like isentropic slopes) that appears in diffusivity theories and the surface variables of the EBM. A general expression for meridional contrast-dependent diffusivity is then a power-law function of T_2 and h_2 relative to their control values:

$$\mathcal{D}(T_2, h_2) = \overline{\mathcal{D}}\left(\frac{T_2}{\overline{T}_2}\right)^n \left(\frac{h_2}{\overline{h}_2}\right)^m. \tag{3}$$

As the exponent is raised, the sensitivity of the diffusivity to the contrast increases. For example, a weakened temperature gradient relative to that of the control climate, $T_2/\overline{T}_2 < 1$, implies a larger reduction of $\mathcal{D}$ from the control $\overline{\mathcal{D}}$ if $n > 0$ and n is large. Again, we emphasize that the T_2 or h_2 dependence is modifying the magnitude of the spatially uniform diffusivity and does not, for example, give it a specific form of spatial dependence. The opportunities and challenges to extend to spatially varying diffusivities will be discussed in section 5.

The control value of the spatially constant diffusivity is $\overline{\mathcal{D}} = 0.3\,\mathrm{W\,m^{-2}\,K^{-1}}$ chosen to give an Earth-like climate when $\mathcal{F} = 0$. This gives the control numerical solution that has a global-mean surface temperature of 288.6 K and an equator-to-pole difference of 46.5 K. The second-order Legendre polynomial component of the temperature $\overline{T}_2$ is −29.3 K and of the MSE $\overline{h}_2$ is −65.4 K, which are negative because both decrease from equator to pole. These values will be used as the control values to study the solutions for climate-state-dependent diffusivities, except for where we assess the sensitivity to the choice of the value of $\overline{\mathcal{D}}$ in the climate-invariant diffusivity case.

b. *Analytic approach and numerical results for climate-invariant diffusivity*

In this section, we briefly review the central theoretical result of MH18 and show the numerical EBM solution response to radiative forcing for the climate-state-independent diffusivity moist EBM.

To derive analytic EBM theories for the pattern of temperature change, we follow the approach of MH18, who built on dry EBM theories (North 1975; North et al. 1981). The governing equation is expanded spectrally in Legendre polynomials and truncated to find solutions. The global-mean (zero-order polynomial) and second-order Legendre polynomial component are assumed to account for much of the meridional structure of the temperature change pattern (sometimes known as a "two-mode solution"). MH18 presented these analytic solutions for moist EBMs with climate-invariant diffusivity.

The essence of MH18's analytic approach for moist EBMs is to approximate the MSE h in terms of temperature T via Taylor series expansion. This expansion can be done about a spatially varying climatological surface temperature distribution [MH18's Eq. (12)] or about the global-mean surface temperature [MH18's Eq. (14)]. Here, we adopt the latter approach. It is simpler, makes analysis feasible, and the error it introduces is modest.

Our approximate MSE $\tilde{h}$ is defined as

$$\tilde{h} \equiv T + L\mathcal{H}c_p^{-1}[q^*(T_0) + \partial_T q^*|_{T_0}(T - T_0)]. \tag{4}$$

The appeal of linearizing the definition of q^* about the global-mean temperature T_0 rather than the spatially varying climatology is that it eliminates the spatial derivatives of the linearized q^*: $\partial_x \tilde{h} = (1 + L\mathcal{H}c_p^{-1}\partial_T q^*|_{T_0})\partial_x T$. After inserting this definition of MSE $h = \tilde{h}$ into the steady-state EBM governing equation Eq. (1), we have

$$0 = \frac{1}{4}QSa - (A + BT) - \partial_x[\mathcal{D}(1 + L\mathcal{H}c_p^{-1}\partial_T q^*|_{T_0})(1 - x^2)\partial_x T] + \mathcal{F}. \tag{5}$$

So, we can think of the role of latent energy as changing the magnitude of the diffusivity. That is, diffusing along the MSE gradient with $\mathcal{D}$ in Eq. (1) is approximated by diffusing along the temperature gradient with an effective diffusivity $\mathcal{D}(1 + L\mathcal{H}c_p^{-1}\partial_T q^*|_{T_0})$ in Eq. (5). Collecting terms at second

order and specifying the climate-state-independent diffusivity $\mathcal{D} = \overline{\mathcal{D}}$, we have

$$T_2 = \frac{\frac{1}{4}Q(Sa)_2}{6\overline{\mathcal{D}}(1 + L\mathcal{H}c_p^{-1}\partial_T q^*|_{T_0}) + B}, \tag{6}$$

where the factor of 6 results from the eigenvalue of the eigenfunction for the diffusion operator. This expression shows that the climatological T_2 is negative because the numerator is negative: there is less absorbed solar radiation in the high latitudes than the low latitudes. Under global warming, the latent-energy-dependent term $(1 + L\mathcal{H}c_p^{-1}\partial_T q^*|_{T_0})$ increases with T_0 according to the CC relation. This increases the effective diffusivity and reduces the magnitude of T_2, implying a polar-amplified warming. The T_0 dependence here is fundamental to the polar-amplified warming in this moist EBM with approximate MSE [i.e., Eq. (5)]. If $\partial_T q^*$ is independent of temperature, there is nothing in Eq. (6) that varies with climate and T_2 would always remain unchanged. More generally, if $\mathcal{H} = 0$ for a dry atmosphere or $\overline{\mathcal{D}} = 0$ for the radiative equilibrium, T_2 becomes independent of T_0 even for the moist EBM with the full MSE definition [i.e., Eq. (1)]. Together, these emphasize the essential role of latent energy transport in polar amplification in moist EBMs.

The sensitivity of this expression to global-mean surface temperature T_0 change can be explicitly obtained with an application of the chain rule in evaluating the derivative of Eq. (6) at the control climate state:

$$\left.\frac{\partial T_2}{\partial T_0}\right|_{\overline{T}} = \frac{-6\overline{\mathcal{D}}\,\overline{T}_2 L\mathcal{H}c_p^{-1}\partial_{TT}q^*|_{\overline{T}_0}}{6\overline{\mathcal{D}}(1 + L\mathcal{H}c_p^{-1}\partial_T q^*|_{\overline{T}_0}) + B}, \tag{7}$$

where the left-hand side depends on $\overline{T}$ via the $\overline{T}_0$ and $\overline{T}_2$ components that appear on the right-hand side. This expression is similar to Eq. (14) of MH18, who gave numerical values for representative values of Earth that imply about 2.8 times as much warming at the pole relative to the equator. [There is a modest difference in that their Eq. (14) required an integral to compute a modification of the diffusivity due to latent energy that appears in that denominator, but it has a similar numerical value as the product of the term in parentheses, $(1 + L\mathcal{H}c_p^{-1}\partial_T q^*|_{\overline{T}_0})$, in the denominator here.] One can see that this equation has a positive-definite denominator and numerator ($\overline{T}_2 < 0$; all other terms > 0). Therefore, $\partial_{T_0} T_2|_{\overline{T}} > 0$ and there is always a reduction of the magnitude of T_2 with warming. That is, the temperature gradients weaken with warming, regardless of the parameter values used to evaluate the expression.

Another appeal of adopting the approximate MSE $h = \tilde{h}$ in Eq. (4) is that we can also derive the analytic expression for the sensitivity of MSE contrast h_2 to T_0 change. Using Eq. (4), we can simply express

$$h_2 = (1 + L\mathcal{H}c_p^{-1}\partial_T q^*|_{T_0})T_2 \tag{8}$$

and apply the product rule to obtain the relationship between h_2 and T_2 sensitivities:

$$\frac{\partial h_2}{\partial T_0} = (1 + L\mathcal{H}c_p^{-1}\partial_T q^*|_{T_0})\frac{\partial T_2}{\partial T_0} + T_2 L\mathcal{H}c_p^{-1}\partial_{TT}q^*|_{T_0}. \tag{9}$$

Evaluating this at the control climate state and inserting the $\partial_{T_0} T_2|_{\overline{T}}$ expression in Eq. (7) into it gives

$$\left.\frac{\partial h_2}{\partial T_0}\right|_{\overline{T}} = \frac{\overline{T}_2 L\mathcal{H}c_p^{-1}\partial_{TT}q^*|_{\overline{T}_0} B}{6\overline{\mathcal{D}}(1 + L\mathcal{H}c_p^{-1}\partial_T q^*|_{\overline{T}_0}) + B}. \tag{10}$$

Similar to Eq. (7), one can see that this equation is negative definite. That is, $\partial_{T_0} h_2|_{\overline{T}} < 0$ and the MSE gradients always enhance with warming. Given that $\mathcal{D} = \overline{\mathcal{D}}$ is assumed climate invariant, this also guarantees an increased poleward energy transport, which was argued as the essential driver for polar amplification in moist EBMs (with spatially uniform feedbacks and forcing) as discussed above and by MH18. For the same reason, MH18 concluded that applying the uniform MSE increase approximation of Byrne and O'Gorman (2013) over all latitudes cannot be a self-consistent solution in this EBM formulation.

The estimate from these approximate analytic expressions and the numerical solution is compared in Fig. 1a, which shows the pattern of the temperature change with $\mathcal{F} = 3.6\,\mathrm{W\,m^{-2}}$. This radiative forcing corresponds to a global mean temperature change $\Delta T_0 = T_0 - \overline{T}_0 = \mathcal{F}/B = 2\,\mathrm{K}$ (where Δ indicates the difference from the control climate value). The theoretical estimate for the pattern of the temperature change is calculated as $\Delta T_0(1 + \partial_{T_0} T_2|_{\overline{T}})$ from Eq. (7) (Fig. 1a, dashed lines) and is seen to generally track the numerical solution calculated by integrating Eq. (1), the EBM governing equation (solid lines). For the control value of $\overline{\mathcal{D}} = 0.3\,\mathrm{W\,m^{-2}\,K^{-1}}$ used in MH18 and this study, the theory modestly underestimates the T_2 component of the warming (black lines), as also indicated by its slight overestimate of ΔT_2 in Fig. 1b. Likewise, there is a small discrepancy between the numerical solution and Eq. (10) times ΔT_0 for the Δh_2 value that can be seen in Fig. 1d.

Since $\overline{\mathcal{D}} = 0.3\,\mathrm{W\,m^{-2}\,K^{-1}}$ is chosen to give an Earth-like control climate, it is worth studying how sensitive the result is to the choice of $\overline{\mathcal{D}}$ (e.g., Fig. 4 of Armour et al. 2019). For larger $\overline{\mathcal{D}}$, we see that the theoretical estimate does a decent job in predicting the numerical solution for the warming pattern (e.g., yellow lines in Fig. 1a), ΔT_2 (Fig. 1b), and Δh_2 (Fig. 1d). The theory is less successful for smaller $\overline{\mathcal{D}}$ values where the climatological equator-to-pole temperature contrast becomes larger. Since the global-mean temperature is independent of $\overline{\mathcal{D}}$ value, a larger temperature contrast also requires higher tropical temperatures (exceeding 305 K in the three simulations with lowest diffusivity). At these temperatures, linearizing the saturation thermodynamics about the global-mean temperature becomes inadequate because of the CC nonlinearity. Our theory based on the approximate MSE [i.e., Eq. (4)] therefore starts to deviate more from the numerical solutions.

Interestingly, the numerical solutions of the smaller $\overline{\mathcal{D}}$ cases also show a warming pattern that has more warming in the extratropics than the tropics, but is no longer truly polar-amplified because the maximum temperature increase is near 60° latitude (e.g., pink lines in Fig. 1a), indicating contributions from higher-order

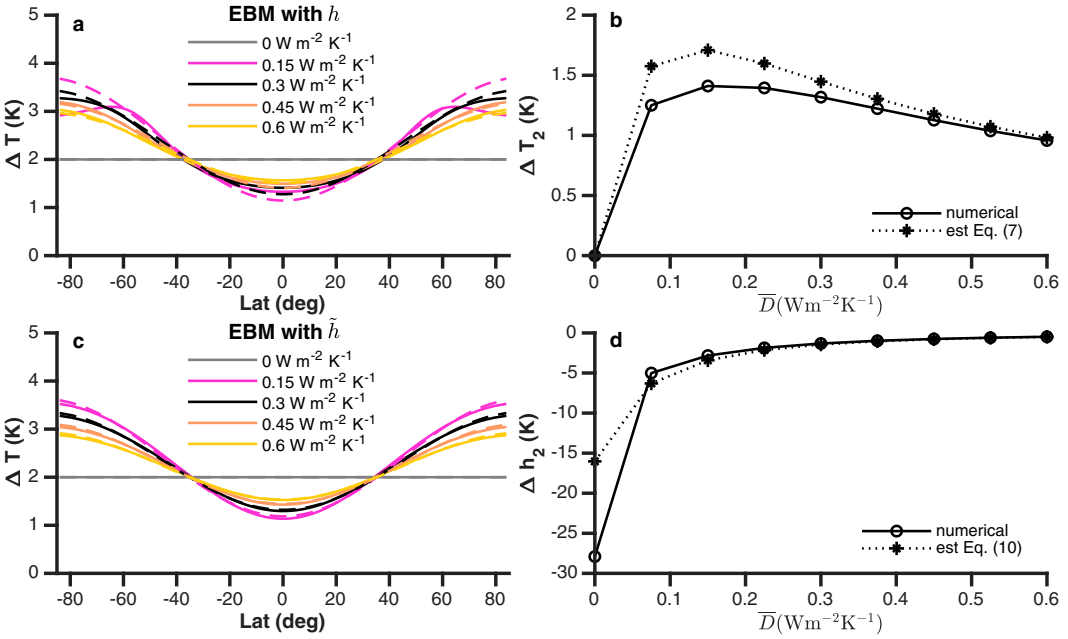

FIG. 1. EBM solutions with climate invariant diffusivity. (a) Change in surface temperature ΔT vs latitude for numerical solutions [Eq. (1); solid lines] and analytic theory (dashed lines) for different values of control diffusivity $\overline{\mathcal{D}}$ indicated in the legend. (b) Change in the second-order Legendre polynomial component of temperature ΔT_2 vs $\overline{\mathcal{D}}$ for numerical solutions [Eq. (1)] and the analytic theory [Eq. (7) scaled by the global-mean temperature change ΔT_0]. (c) As in (a), but for the numerical solutions for the EBM with the linearized MSE approximation, Eq. (5). (d) As in (b), but for the change in the second-order Legendre polynomial component of MSE Δh_2 and the analytic theory [Eq. (10) scaled by ΔT_0]. See section 2b of the text for the detailed calculations of the theoretical estimates for ΔT in (a) and (c).

Legendre components. Many of these higher-order contributions disappear when we numerically integrate Eq. (5), that is, the version of EBM governing equation directly using the MSE approximation (Fig. 1c). Here, the relatively small discrepancy between the numerical solution and theoretical estimate is solely contributed from the projection of the prescribed shortwave, $QS(x)a(x)/4$, on the higher-order Legendre polynomials. Comparing the results of EBM solutions with full versus approximate MSE (Figs. 1a,c) thus suggests that the usefulness of our theory is mostly set by the extent to which the MSE approximation holds. We conclude that the value of $\overline{\mathcal{D}}$ has to be large enough for the solutions to show a robust polar-amplified warming and for the theory to provide reasonable estimates. Fortunately, the Earth-like value, $\overline{\mathcal{D}} \approx 0.3\,\mathrm{W\,m^{-2}\,K^{-1}}$, does fall into this regime, which allows us to make use of the theory to obtain some physical insights in the following.

Having set up the definition of linearized approximate MSE and the spectrally truncated solutions that we will use in subsequent analysis, reviewed the result of MH18 for climate-invariant diffusivity, and quantified the limitation of the theory, we turn to the climate-state-dependent diffusivity formulations.

3. Global-mean temperature-dependent diffusivity

Given that the moist EBM theory with constant diffusivity has polar-amplified warming, we investigate how it would change with a global-mean temperature-dependent diffusivity [Eq. (2)]: $\mathcal{D} = \mathcal{D}(T_0)$.

a. Numerical results

We show the numerical solutions of the surface temperature change using a global-mean temperature-dependent diffusivity Eq. (2) in Fig. 2a (solid lines). As replotted from Fig. 1a, the typical, climate-state-independent diffusivity $\gamma = 0$ has polar-amplified warming with about 2.5 times as much polar warming as in the global mean (black line in Fig. 2a). Increased diffusivity with warming ($\gamma > 0$; blue line in Fig. 2a) has further enhanced polar warming. As the diffusivity is decreased with warming, there is less enhancement of the polar warming (progressively darker shades of solid red lines in Fig. 2a are more negative γ). There is a transition from polar to tropically amplified warming that occurs with a diffusivity that decreases with global-mean surface temperature somewhere between the -2% and -4% K^{-1} cases plotted. We also note that these solutions that have the strongest reductions in the diffusivity with warming show weak spatial variations in the warming pattern from the equator to near 40° latitude and a subsequent steep drop in temperature. This is an indication that there is a higher-order Legendre-polynomial component of the temperature change.

The corresponding changes of surface MSE are shown in Fig. 2c. The climate-invariant diffusivity $\gamma = 0$ has a slightly

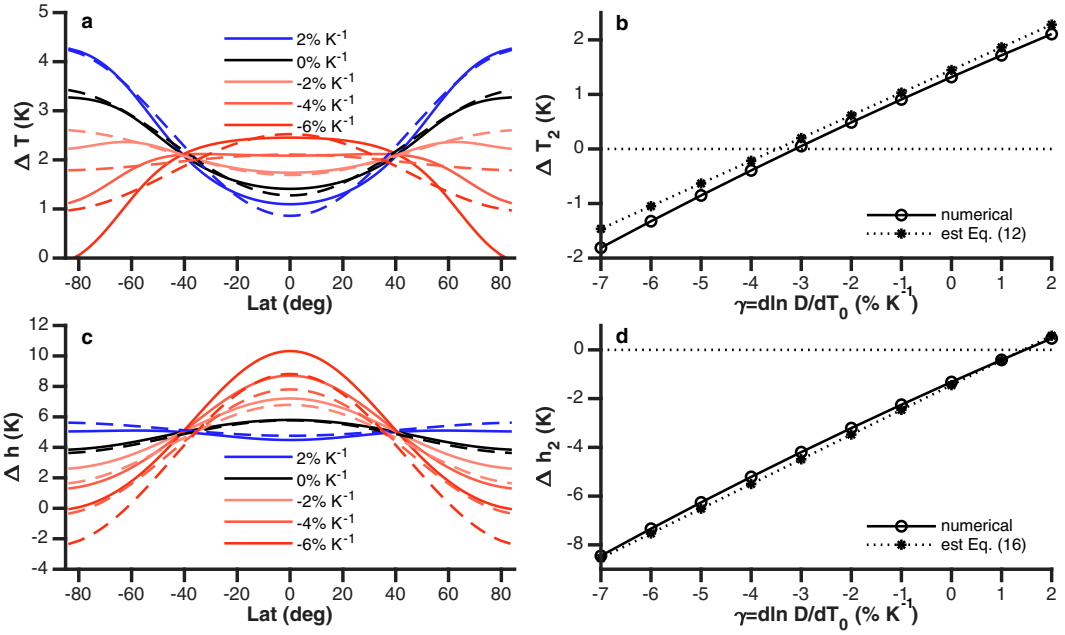

FIG. 2. EBM solutions with global-mean temperature-dependent diffusivity [Eq. (2)]. (a) Change in temperature ΔT vs latitude for numerical solutions [Eq. (1); solid lines] and analytic theory (dashed lines) for different values of diffusivity sensitivity coefficient γ indicated in the legend. (b) ΔT_2 vs γ for numerical solutions [Eq. (1)] and the analytic theory [Eq. (12) scaled by ΔT_0]. (c) As in (a), but for Δh. (d) As in (b), but for Δh_2 and the analytic theory [Eq. (16) scaled by ΔT_0]. See section 3b of the text for the detailed calculations of the theoretical estimates for ΔT in (a) and Δh in (c).

increased equator-to-pole MSE contrast, which is further enhanced with decreasing γ (red lines in Fig. 2c). On the other hand, increasing γ can lead to a reduction of MSE contrast (blue lines in Fig. 2c), with the transition occurring between the 0% and 2% K^{-1} cases plotted.

Since our theoretical developments focus on the sensitivity of the second-order Legendre components, we also compute the values of ΔT_2 and Δh_2 for the numerical solutions in Figs. 2b and 2d. Figure 2b shows the numerical EBM's ΔT_2 in circles against the diffusivity's temperature sensitivity γ. As γ becomes more negative, ΔT_2 decreases approximately linearly. We see here that the transition from positive ΔT_2 (polar-amplified warming) to negative ΔT_2 (tropically amplified warming) occurs near $\gamma = -3\%\ K^{-1}$.

Figure 2d shows the numerical EBM Δh_2 in circles versus γ. For most of the values of γ explored, Δh_2 is negative. Consistent with Fig. 2c, this indicates an increased meridional MSE contrast. The exception occurs for the largest magnitude increase in diffusivity with global-mean temperature. Overall, the response of h_2 to warming varies approximately linearly in γ, which the theory that we derive next can account for.

b. Theory

The start of the analysis proceeds as in section 2b. The EBM governing equation now becomes Eq. (5) with $\mathcal{D}(T_0)$ defined by Eq. (2). Compared to the $\mathcal{D} = \overline{\mathcal{D}}$ solution for the T_2 component of temperature in Eq. (6), the $\mathcal{D} = \mathcal{D}(T_0)$ solution now has an additional modification to the diffusivity in the denominator (beyond the one from the latent energy component of the MSE) that results from its own T_0 dependence:

$$T_2 = \frac{\frac{1}{4}Q(Sa)_2}{6\overline{\mathcal{D}}\{[1 + \gamma(T_0 - \overline{T}_0)](1 + L\mathcal{H}c_p^{-1}\partial_T q^*|_{\overline{T}_0})\} + B}. \quad (11)$$

Relative to Eq. (6), this additional T_0-dependent term in the denominator of Eq. (11) that results from the temperature-dependent diffusivity gives rise to a new term in the numerator of the expression for the T_2 sensitivity to a global-mean temperature change:

$$\left.\frac{\partial T_2}{\partial T_0}\right|_{\overline{T}} = \frac{-6\overline{\mathcal{D}}\,\overline{T}_2[L\mathcal{H}c_p^{-1}\partial_{TT}q^*|_{\overline{T}_0} + \gamma(1 + L\mathcal{H}c_p^{-1}\partial_T q^*|_{\overline{T}_0})]}{6\overline{\mathcal{D}}(1 + L\mathcal{H}c_p^{-1}\partial_T q^*|_{\overline{T}_0}) + B}. \quad (12)$$

This theory is compared to the numerical EBM solutions in Figs. 2a and 2b. The theoretical estimate computed as $\Delta T_0(1 + \partial_{T_0} T_2|_{\overline{T}})$ from Eq. (12) compares less promisingly latitude by latitude as γ decreases due to the presence of higher-order Legendre components (dashed vs solid lines in Fig. 2a). However, it pretty well captures the linear γ dependence of ΔT_2 (Fig. 2b).

The theory has a critical diffusivity sensitivity $\gamma = \gamma_{c,T}$ for which there is no change in T_2 with global warming ΔT_0. This

is the boundary between simulations with polar-amplified and tropically amplified warming. Setting the quantity in square brackets in Eq. (12) to zero results in

$$\gamma_{c,T} = -\frac{L\mathcal{H}c_p^{-1}\partial_{TT}q^*|_{\overline{T}_0}}{1 + L\mathcal{H}c_p^{-1}\partial_T q^*|_{\overline{T}_0}}. \tag{13}$$

For the control values, this expression suggests a critical diffusivity sensitivity of $\gamma_{c,T} \approx -3\%\ \mathrm{K}^{-1}$. Consistent with our theory, the numerical EBM's ΔT_2 changes from positive (polar amplified) to negative (tropically amplified) for $\gamma < -3\%\ \mathrm{K}^{-1}$ (Fig. 2b).

We offer two related interpretations for the form and climatological dependence of $\gamma_{c,T}$. One is mathematical and one is physical. Mathematically, the above expression involves the first and second derivative of the saturation specific humidity with respect to temperature. We can make an approximation and assume a pure exponential form of $q^* = q_0^* \exp(\alpha T)$, where α is the CC sensitivity of $\approx 7\%\ \mathrm{K}^{-1}$. Then, we have an expression for $\gamma_{c,T}$ of the form

$$\gamma_{c,T} \approx -\frac{\kappa\alpha^2}{1 + \kappa\alpha} > -\alpha, \tag{14}$$

where $\kappa = L\mathcal{H}c_p^{-1}q^*|_{\overline{T}_0}$. This expression for the magnitude of $\gamma_{c,T}$ is bound from above by the CC sensitivity α.

A physical picture of what controls $\gamma_{c,T}$ can be again obtained by considering the role of latent energy in the total transport as in section 2b. As discussed for the $\mathcal{D} = \overline{\mathcal{D}}$ case there, the theory suggests that T_2 changes with T_0 due to the latent-energy-dependent term $(1 + L\mathcal{H}c_p^{-1}\partial_T q^*|_{T_0})$ which modifies the effective diffusivity in Eq. (6). For the $\mathcal{D} = \mathcal{D}(T_0)$ case here, Eq. (11) suggests that an additional T_0 dependence from $\mathcal{D} = \mathcal{D}(T_0)$ can counteract the T_0 dependence from the latent-energy-dependent term to keep the effective diffusivity and T_2 unchanged if γ is

$$\begin{aligned}\gamma_{c,T} &= -\frac{\partial \ln(1 + L\mathcal{H}c_p^{-1}\partial_T q^*|_{T_0})}{\partial T_0}\bigg|_{\overline{T}} \\ &= -\left(\frac{L\mathcal{H}c_p^{-1}\partial_T q^*|_{\overline{T}_0}}{1 + L\mathcal{H}c_p^{-1}\partial_T q^*|_{\overline{T}_0}}\right)\frac{\partial_{TT}q^*|_{\overline{T}_0}}{\partial_T q^*|_{\overline{T}_0}}\end{aligned} \tag{15}$$

The last expression indicates that $\gamma_{c,T}$ is set by the relative contribution of latent energy component to the MSE gradient, the term in parentheses, and the temperature dependence of the saturation specific humidity constrained by the CC relation. The latter is again α if we adopt the exponential approximation discussed above. This suggests that the prefactor of α is set by how much MSE gradient is from the latent component in the control climate. The more dominant the latent energy gradient is, the more the diffusivity has to decrease to fight against the increase of latent energy transport to prevent polar-amplified warming.

Next, we use the theory for T_2 to quantify MSE contrasts. As for Eq. (10), but inserting the $\partial_{T_0} T_2|_{\overline{T}}$ expression of Eq. (12) into Eq. (9) gives

$$\begin{aligned}\frac{\partial h_2}{\partial T_0}\bigg|_{\overline{T}} &= \frac{\overline{T}_2 L\mathcal{H}c_p^{-1}\partial_{TT}q^*|_{\overline{T}_0}}{6\overline{\mathcal{D}}(1 + L\mathcal{H}c_p^{-1}\partial_T q^*|_{\overline{T}_0}) + B} \\ &\quad \times \left[B + 6\overline{\mathcal{D}}(1 + L\mathcal{H}c_p^{-1}\partial_T q^*|_{\overline{T}_0})\frac{\gamma}{\gamma_{c,T}}\right].\end{aligned} \tag{16}$$

This theory is compared to the numerical EBM solutions in Figs. 2c and 2d. The theoretical estimate is computed as Δh_0 plus Eq. (16) times ΔT_0, with $\Delta h_0 = \Delta T_0 + L\mathcal{H}c_p^{-1}[q^*(T_0 + \Delta T_0) - q^*(T_0)]$ from Eq. (4). Since Δh_0 becomes an underestimation when the equator-to-pole temperature contrast is large with warmer tropics, our theoretical estimate of the MSE changes is constantly lower than the numerical solution for the negative γ cases (red lines in Fig. 2c). However, even for these cases, the theory captures the spatial pattern very well as it is dominated by the second-order Legendre component. Consistently, there is a good agreement between the theory and numerical solution of Δh_2 and one can see that a state of no change in MSE contrast is obtained if the diffusivity increases by $\approx 1.5\%\ \mathrm{K}^{-1}$ (Fig. 2d). This corresponds to another critical diffusivity sensitivity

$$\gamma_{c,h} = -\frac{B}{6\overline{\mathcal{D}}(1 + L\mathcal{H}c_p^{-1}\partial_T q^*|_{\overline{T}_0})}\gamma_{c,T}, \tag{17}$$

which sets the sum of the terms in square brackets of Eq. (16) to zero. For the climatological values, the ratio of B to $6\overline{\mathcal{D}}(1 + L\mathcal{H}c_p^{-1}\partial_T q^*|_{\overline{T}_0})$ is about one-half, so $\gamma_{c,h} \approx +1.5\%\ \mathrm{K}^{-1}$ produces a state of approximately unchanged MSE contrast. Physically, this ratio represents the relative efficiency of the system to damp an imposed radiative forcing via OLR locally or through the meridional spread by diffusive transport. The less efficient the OLR relative to the diffusive transport, the more the anomalous MSE contrast is smoothed out by the turbulent diffusion and the less h_2 changes.

As noted in section 2b, MH18 presented an estimate for polar amplification inspired by Byrne and O'Gorman (2013) that assumed uniform Δh at all latitudes and determined the warming pattern to achieve that state. There, they noted that this solution does not satisfy the energy balance of climate-state invariant diffusivity moist EBM [i.e., Eq. (10)], as it would require an unchanged energy transport. Here, we see that a uniform Δh can satisfy the EBM equation if diffusivity changes with global-mean temperature in this specific way. This unchanged h_2 warmed climate has large increases in T_2 (substantially enhanced transport and the concomitantly large polar-amplified warming) and helps build intuition for some of the climate-state-dependent diffusivities that depend on gradients considered in the next section.

4. Temperature and energy gradient-dependent diffusivity

In this section, we present numerical results and analytic theory for diffusivities that depend on either or both of the second-order Legendre polynomial component of temperature and MSE [Eq. (3)]: $\mathcal{D} = \mathcal{D}(T_2, h_2)$. The exponent n controls

the T_2 dependence of the diffusivity and the exponent m controls the h_2 dependence of the diffusivity. We consider $m = 0$ and vary n to examine how this representation of temperature contrast-dependent diffusivity affects the EBM solution, as well as the case with diffusivity dependent solely on MSE contrast ($n = 0$ with varied m). Last, we examine the case of combined dependence with equal exponents ($n = m$).

We note that the analytic EBM theory developed in the following is general, so the previous literature is largely used to shape our choices of parameters for the calculations of numerical EBM solutions. Our overview here sets aside the exact definitions for how the temperature or MSE gradients are evaluated and focuses on the power laws: Frierson et al. (2007) proposed that $\mathcal{D}$ scales with the 3/2 power of the temperature gradient [their Eq. (A6)], which suggests $n = 3/2$. Lu et al. (2022) proposed that $\mathcal{D}$ scales with the third power of the temperature gradient [their Eq. (A13a)], which suggests $n = 3$. Chang and Held (2022) generalized the theories of Held and Larichev (1996) and Barry et al. (2002) [their Eq. (29)]. They showed that Held and Larichev's (1996) theory corresponds to a special case of dry atmospheres with the mixing slope approximated by isentropic slope, and an additional constant isentropic slope assumption would suggest $n = 3/2$. For moist atmospheres, they suggest $m = n = 3/2$, if the temperature gradient along the mixing slope is assumed to scale with horizontal temperature gradient, following Barry et al.'s (2002) assumption. Certain choices (e.g., exclusively h_2-dependent diffusivity, $m > 0$ with $n = 0$) have never been suggested, but are useful to build intuition for the roles of the individual components of the combined T_2- and h_2-dependent diffusivity case. In all cases, we consider $m \geq 0$ and $n \geq 0$.

a. Numerical results

Figure 3a shows the temperature change versus latitude for the numerical solution of the EBM with diffusivity dependent on T_2 only ($m = 0$): $\mathcal{D}(T_2)$. We plot select exponents of the power-law dependence ($n = 3/2$ and 3). As the exponent increases from zero (shown in black), there is a reduction in polar-amplified warming. This is expected from the stabilizing feedback: polar amplification provoked initially tends to increase T_2 from its negative control value [i.e., Eq. (7)], and this, in turn, decreases the diffusivity, which reduces the increase in meridional MSE transport that underlies polar amplification in this EBM configuration. Figure 3b shows the systematic variation of the exponent. The corresponding ΔT_2 decreases from ≈1.3 to ≈0.4 K as n increases from 0 to 3 and remains positive in all cases. Our analysis will, indeed, reveal that larger exponents cannot change the sign of ΔT_2. Figure 3f shows the diffusivity decrease is $\approx -2.5\%\ \mathrm{K}^{-1}$ for the highest exponent. Figure 3d shows that h gradients increase with n: the more uniform ΔT, has relatively stronger MSE gradients and this is a countervailing tendency for reduced energy transport as the diffusivity decreases ($\Delta \mathbf{F}_a \sim \overline{\mathcal{D}}\partial_x \Delta h + \Delta \mathcal{D} \partial_x \overline{h}$). A central appeal of the analysis of the next section is that these competing effects are quantitatively captured via the analysis of the EBM's governing equation.

Figure 3c shows the temperature change versus latitude for the numerical solution of the EBM with diffusivity dependent on h_2 only ($n = 0$): $\mathcal{D}(h_2)$. This form of the climate-state-dependent diffusivity has an increase in polar amplification as the exponent increases. Here, the feedback associated with the diffusivity is as follows: the initial response tends to decrease h_2 [more negative relative to the negative $\overline{h}_2$; Eq. (10)], this in turn, increases the diffusivity (Fig. 3f), augmenting the increase in meridional MSE transport that underlies the polar amplification. The higher exponent approaches the uniform Δh limit (Fig. 3d). Figure 3b shows the systematic variation of the exponent, revealing that ΔT_2 reaches ≈1.6 K (about 25% more polar amplification than the climate-state-independent diffusivity). The contrast between the behavior of T_2-dependent diffusivity (orange in Fig. 3) and h_2-dependent diffusivity (purple in Fig. 3) is clear: one has decreased diffusivity and weakened polar amplification and the other has increased diffusivity and enhanced polar amplification. This is suggestive that the combined case has more muted changes as a result of these competing effects.

Figure 3e shows the temperature change versus latitude for the numerical solution of the EBM with diffusivity dependent on both T_2 and h_2: $\mathcal{D}(T_2, h_2)$ and $m = n$. This form of the climate-state-dependent diffusivity has a modest decrease in polar amplification as the exponent increases (brown circles in Fig. 3b). For $m = n = 3/2$, ΔT_2 is ≈1.1 K (about 20% less polar amplification than the climate-state-independent diffusivity). There is a modest increase in meridional MSE gradient and a modest decrease in diffusivity as the exponents increase (Figs. 3d,f). These subtle effects result from the competing roles of T_2 versus h_2 dependency of diffusivity and provide a stringent test for the theory developed in the next section.

b. Theory

Here, we derive the general case of the EBM solution for diffusivities that depend on the combined T_2, h_2-dependent diffusivity [Eq. (3)]. Theories for the individual diffusivity dependencies can be recovered by setting the relevant exponent to zero [e.g., theory for $\mathcal{D}(T_2)$ is given by $m = 0$].

The starting point is, as before, the second-order Legendre polynomial truncation of the EBM governing equation. The approximate definition of MSE $\tilde{h}$ allows us to replace h_2 in the $\mathcal{D}(T_2, h_2)$ expression in Eq. (3) using Eq. (8). Setting $\mathcal{D}$ in Eq. (5) with this expression and collecting terms at second order results in

$$0 = \frac{1}{4}Q(Sa)_2 - BT_2 - 6\overline{\mathcal{D}}(1 + L\mathcal{H}c_p^{-1}\partial_T q^*|_{T_0}) \times \left(\frac{1 + L\mathcal{H}c_p^{-1}\partial_T q^*|_{T_0}}{1 + L\mathcal{H}c_p^{-1}\partial_T q^*|_{\overline{T}_0}}\right)^m \left(\frac{T_2}{\overline{T}_2}\right)^{m+n} T_2. \tag{18}$$

Taking the derivative with respective to global-mean temperature T_0 and evaluating at the control climate state, we have

$$\left.\frac{\partial T_2}{\partial T_0}\right|_{\overline{T}} = \frac{-6\overline{\mathcal{D}}\,\overline{T}_2 L\mathcal{H}c_p^{-1}\partial_{TT} q^*|_{\overline{T}_0}(m+1)}{6\overline{\mathcal{D}}(1 + L\mathcal{H}c_p^{-1}\partial_T q^*|_{\overline{T}_0})(m+n+1) + B}. \tag{19}$$

Note that this expression is positive definite, in contrast to the corresponding result for the T_0-dependent diffusivity $\mathcal{D}(T_0)$

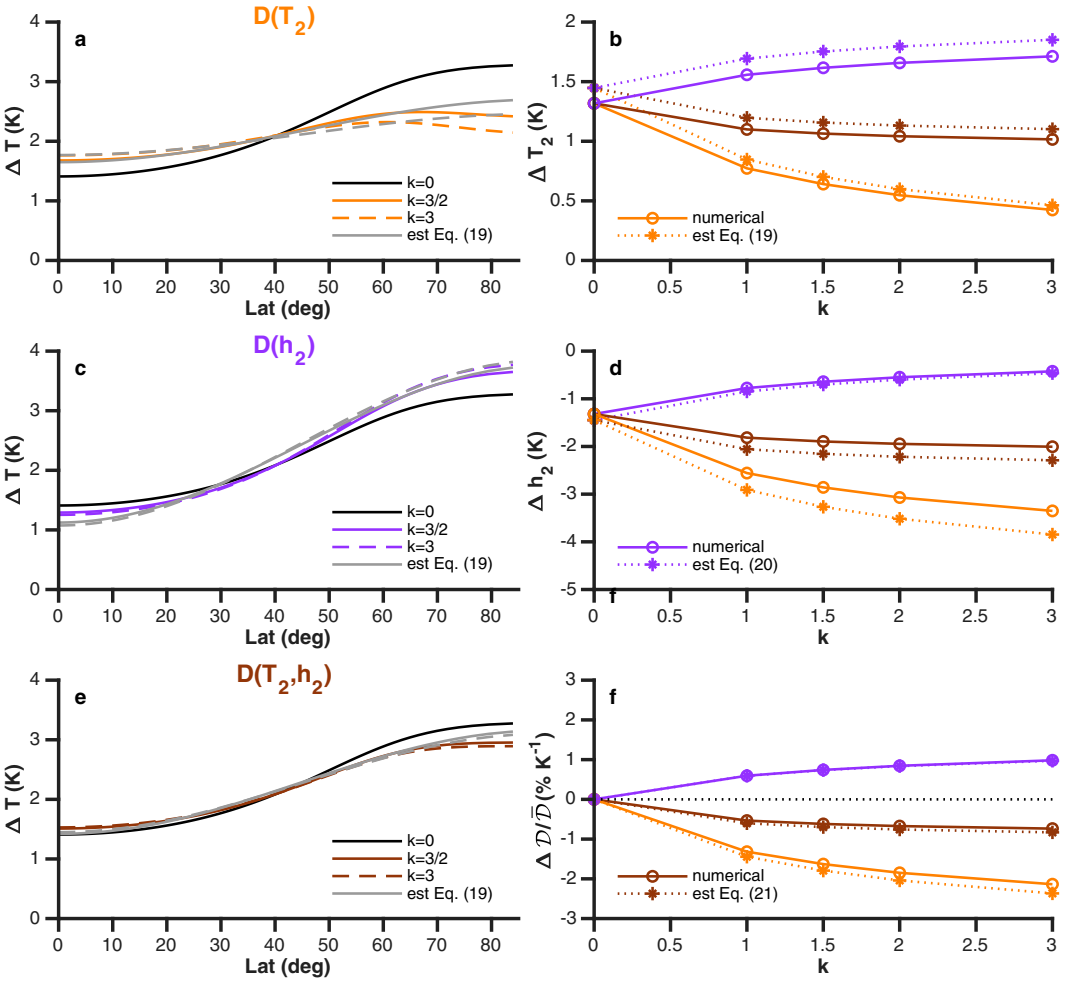

FIG. 3. EBM solutions with T_2- (orange), h_2- (purple), and combined T_2, h_2- (brown) dependent diffusivity [Eq. (3)]. (a),(c),(e) Change in temperature ΔT vs latitude for numerical solutions [Eq. (1); black and colored lines] and analytic theory (gray lines) for different values of exponent k of Eq. (3) indicated in the legend. (b) ΔT_2 vs k for numerical solutions [Eq. (1)] and the analytic theory [Eq. (19) scaled by ΔT_0]. (d) Δh_2 vs k for numerical solutions [Eq. (1)] and the analytic theory [Eq. (20) scaled by ΔT_0]. (f) Percentage change in the diffusivity $\mathcal{D}$ per kelvin vs k for numerical solutions [Eq. (1)] and the analytic theory [Eq. (21)]. See section 4b of the text for the detailed calculations of the theoretical estimates of ΔT in (a), (c), and (e).

[Eq. (12)]. The physical meaning of the positive definite expression is that there are no parameter values for this form of the climate-state-dependent diffusivity that have tropically amplified warming. The limiting case of $n \to \infty$ has $\Delta T_2 \to 0$. That is, polar amplification cannot be eliminated with this diffusivity formulation.

As before, this T_2 sensitivity to T_0 can be used to determine how h_2 varies. When substituting into Eq. (9), we have

$$\left.\frac{\partial h_2}{\partial T_0}\right|_{\overline{T}} = \frac{\overline{T}_2 L\mathcal{H}c_p^{-1}\partial_{TT}q^*|_{\overline{T}_0}[B + 6\overline{\mathcal{D}}(1 + L\mathcal{H}c_p^{-1}\partial_T q^*|_{\overline{T}_0})n]}{6\overline{\mathcal{D}}(1 + L\mathcal{H}c_p^{-1}\partial_T q^*|_{\overline{T}_0})(m + n + 1) + B}. \tag{20}$$

This is a negative definite expression, meaning MSE gradients increase with global mean temperature, for all parameter values. For $m \to \infty$, this expression implies $\Delta h_2 \to 0$.

Last, these T_2 and h_2 sensitivity expressions can also be substituted into the $\mathcal{D}(T_2, h_2)$ formula Eq. (3) to derive a theory for the associated diffusivity sensitivity:

$$\gamma = \left.\frac{\partial \ln \mathcal{D}}{\partial T_0}\right|_{\overline{T}} = \left(\frac{L\mathcal{H}c_p^{-1}\partial_{TT}q^*|_{\overline{T}_0}}{1 + L\mathcal{H}c_p^{-1}\partial_T q^*|_{\overline{T}_0}}\right) \times \left[\frac{Bm - 6\overline{\mathcal{D}}(1 + L\mathcal{H}c_p^{-1}\partial_T q^*|_{\overline{T}_0})n}{6\overline{\mathcal{D}}(1 + L\mathcal{H}c_p^{-1}\partial_T q^*|_{\overline{T}_0})(m + n + 1) + B}\right]. \tag{21}$$

The numerator has a difference between m and n: m tends to increase the diffusivity, while n tends to decrease it. Physically, this corresponds to the counteracting effects of increased MSE gradient Eq. (20) and decreased temperature gradient Eq. (19) on the diffusivity change when T_0 is increased. This competition

between the two gradients was speculated by Chang and Held (2022) to limit the warming response of diffusivity, and to explain how some previous studies using constant-diffusivity EBMs can reasonably emulate comprehensive GCM simulations. The analytic EBM theory here provides a new quantitative description of this competition.

For the case of equal exponents ($m = n$), the diffusivity decreases since the ratio of B to $6\overline{\mathcal{D}}(1 + L\mathcal{H}c_p^{-1}\partial_T q^*|_{\overline{T}_0})$ is about one-half for Earth-like parameter values, as discussed before. On the other hand, the upper and lower bounds of the diffusivity sensitivity can be obtained by considering two limiting cases. For $m = 0$ and $n \to \infty$, $\Delta T_2 \to 0$ and $\gamma \to \gamma_{c,T}$. For $n = 0$ and $m \to \infty$, $\Delta h_2 \to 0$ and $\gamma \to \gamma_{c,h}$. Therefore, for $m \geq 0$ and $n \geq 0$, $\gamma_{c,T} < \gamma < \gamma_{c,h}$ is bounded by the two critical diffusivity sensitivities [Eqs. (13) and (17)] discussed in section 3b.

Figure 3 has comparisons of these theories with the numerical EBM solutions. There is some discrepancy in meridional structure of temperature changes, as the numerical solution has some higher-order components that the theory, estimated as $\Delta T_0(1 + \partial_{T_0} T_2|_{\overline{T}})$ from Eq. (19), cannot capture (gray vs colored lines in Figs. 3a,c,e). There is also systematic biases for the theoretical estimated ΔT_2 [Eq. (19)] and Δh_2 [Eq. (20)] compared to the numerical solutions (dotted vs solid lines in Figs. 3b,d). Overall, the errors of the theory are about 10% for ΔT_2 and are about 15% for Δh_2. On the other hand, the numerical solutions' diffusivity changes are well explained by the theory [Eq. (21)] in all cases (Fig. 3f).

5. Discussion

There are some combinations of the moist EBM coefficients (e.g., B, $\mathcal{D}$, and temperature derivatives of q^*) that appear repeatedly in the new analytic formulas. In this section, we introduce two key parameters that encapsulate the EBM theory, shedding light on the origin of the sensitivities derived from the theories and helping to connect them with the theories proposed by previous studies.

First, the relative roles of radiative restoring versus advective restoring of local energy flux anomalies (two terms with feedback units of W m^{-2} K^{-1}) is given by μ:

$$\mu \equiv \frac{B}{6\overline{\mathcal{D}}(1 + L\mathcal{H}c_p^{-1}\partial_T q^*|_{\overline{T}_0})}\bigg|_{\overline{T}} = \frac{B}{6\overline{\mathcal{D}}(1 + L\mathcal{H}c_p^{-1}\partial_T q^*|_{\overline{T}_0})}. \tag{22}$$

It is introduced as it measures the relative importance of the only two energy flux restoring terms that depend on temperature in the climatological local energy balance. The climatological dependence $\overline{(\cdot)}$ is applied to the latent-energy-dependent term $(1 + L\mathcal{H}c_p^{-1}\partial_T q^*|_{\overline{T}_0})$, since it is the only parameter in our moist EBM governing equation with the approximate MSE [i.e., Eq. (5)] that is climate-state dependent.

The second parameter (in units of K^{-1}) is

$$\chi \equiv \frac{\partial \ln(1 + L\mathcal{H}c_p^{-1}\partial_T q^*|_{\overline{T}_0})}{\partial T_0}\bigg|_{\overline{T}} = \frac{L\mathcal{H}c_p^{-1}\partial_{TT} q^*|_{\overline{T}_0}}{1 + L\mathcal{H}c_p^{-1}\partial_T q^*|_{\overline{T}_0}}, \tag{23}$$

which is introduced as we are interested in the sensitivity to global-mean temperature change and again the factor $(1 + L\mathcal{H}c_p^{-1}\partial_T q^*|_{\overline{T}_0})$ marks the only nonlinear temperature-dependent term in the governing equation, which fundamentally gives rise to the sensitivity to T_0 in our moist EBMs.

The sensitivities of T_2, h_2, and $\mathcal{D}$ derived so far can all be recast into functions of μ and χ (see the appendix). For instance, the two critical diffusivity sensitivities defined in Eqs. (13) and (17) are $\gamma_{c,T} = -\chi$ and $\gamma_{c,T} = \mu\chi$, respectively. We have provided physical interpretations for them in the above sections, and expressing them in terms of the two key parameters offers an even more parsimonious way to reveal the essential physics.

An advantage of recasting our results in terms of these key parameters is that we can more easily compare our theories to Frierson et al. (2007). Frierson et al. (2007) developed moist EBM theories with climate-state-dependent diffusivities to explain the results of a series of idealized GCM simulations where the saturation vapor pressure is modified by a multiplicative factor ξ. This is analogous to replacing q^* by ξq^* in Eq. (1). Assuming a diffusivity that depends on temperature gradient, they showed that their EBM could capture the combination of weakened temperature gradient, decreased diffusivity, and increased poleward energy transport as ξ is increased in their GCM simulations. Despite using a different OLR formulation, our EBM theories can offer qualitatively similar predictions for the sensitivities of these aspects of the climates generated by manipulating ξ. The sensitivities to ξ can be obtained by simply replacing χ with $\partial_\xi \ln(1 + L\mathcal{H}c_p^{-1}\partial_T \xi q^*|_{\overline{T}_0})|_{\overline{T}}$ in the theory derived in section 4b (see also appendix) with $m = 0$. So long is this alternative χ remains positive, we recover weakened temperature gradients (increased T_2) and reduced $\mathcal{D}$, while the increase in MSE gradients (decreased h_2) is sufficient to increase the poleward transport as ξ is increased. Frierson et al. (2007) also noted that the poleward transport in fact barely changed with ξ as the OLR in their gray radiation formulation is insensitive to surface temperature changes. In our theories with a linear OLR formulation, this is analog to approaching the $B = \mu = 0$ limit, where the sign of all sensitivities remains the same.

The critical diffusivity sensitivity for the uniform temperature increase $\gamma_{c,T} = -\chi$ has in fact also been derived in Shaw and Voigt (2016). Shaw and Voigt (2016) considered a uniform warming $\Delta T_2 = 0$ and used the approximate MSE definition [their Eq. (3)], which is the same as ours, to derive the corresponding MSE transport [their Eq. (5)]. This can be recovered by Eq. (9) with $\partial_{T_0} T_2 = 0$, which gives $\partial_{T_0} h_2|_{\overline{T}} = \overline{h}_2\chi$ when evaluated at the control climate state. They next assumed an unchanged energy transport $\Delta(\mathcal{D}h_2)|_{\overline{T}} = 0$ and derive the corresponding diffusivity sensitivity to the global mean temperature change [their Eq. (11)]. In our notation, this is $\gamma = \partial_{T_0} \ln\mathcal{D}|_{\overline{T}} = -\partial_{T_0} \ln h_2|_{\overline{T}} = -\chi = \gamma_{c,T}$. The crucial difference between the two derivations is that an unchanged energy transport is a direct result following the $\Delta T_2 = 0$ assumption in our EBM formulation (with a uniform B and $\mathcal{F}$). However, an unchanged energy transport is an independent assumption in Shaw and Voigt (2016), motivated by the numerical results of

previous GCM studies (e.g., Frierson et al. 2007) rather than global energy balance. As shown in Shaw and Voigt's (2016) aquaplanet simulations, neither of the two assumptions hold even if the model is forced with a prescribed uniform sea surface temperature increase, making any quantitative comparison with their theory difficult.

The diffusivity sensitivity derived for that which depends on temperature gradient $\mathcal{D}(T_2)$ [Eq. (21)] offers a quantitative interpretation for the "reductio ad absurdum" argument put forward in Lu et al. (2022, their section 5a). Specifically, they argued that for a uniform radiative forcing and "in the absence of any strong negative feedback over the polar region" the diffusivity must decrease but can only decrease less than "the CC regulated increase of moisture gradient" if the diffusivity depends on temperature gradient. In our theories (which assume a uniform B and $\mathcal{F}$), this is equivalent to setting $m = 0$ in Eq. (21). This states that the diffusivity sensitivity is bounded by $0 > \gamma > \gamma_{c,T} = -\chi$, where the lower bound is the MSE contrast in the limiting case of uniform warming discussed in Shaw and Voigt (2016) and above. As discussed in section 3b, $\gamma_{c,T} = -\chi$ is roughly half of the CC sensitivity, so this is a stricter bound than Lu et al.'s (2022) argument.

Since the diffusivities diagnosed in the GCM simulations vary with latitude (e.g., Fig. 6 of Frierson et al. 2007), it is also fair to ask how our results change with this additional layer of complexity. Following North (1975), our theories can be easily generalized to a spatially varying diffusivity, $\mathcal{D}(x) = \mathcal{D}_0\eta(x)$, if only the global-mean value $\mathcal{D}_0$ is climate-state dependent but its spatial structure $\eta(x)$ is climate invariant. All the sensitivity formulations derived are unaltered except that $\overline{\mathcal{D}}$ in μ is replaced by

$$-\frac{5}{12}\overline{\mathcal{D}}_0\int_{-1}^{1} P_2(x)\partial_x[\eta(x)(1-x^2)\partial_x P_2(x)]dx, \tag{24}$$

where $\overline{\mathcal{D}}_0$ is the control value of the global mean diffusivity. How well the theory compares with the numerical solution then depends on the extra higher-order Legendre components excited by $\eta(x)$, and carrying out these calculations is technically straightforward. However, the central theoretical question that remains is whether a climate invariant $\eta(x)$ is indeed physically justifiable. We note that the functional form of $\eta(x)$ in the EBM studies that incorporate spatially varying diffusivities is often empirically chosen to emulate GCMs (e.g., Lu et al. 2022), which the extension of the theory described here could capture. There is, however, no theoretical reason to expect $\eta(x)$ to stay unchanged in warm climates. If anything, it is also unsettled whether the Hadley cell transport in the tropics can be approximated by diffusion (e.g., Lindzen and Farrell 1980; Mbengue and Schneider 2018; Siler et al. 2018). In addition, the existing diffusivity theories are developed in the homogeneous limit. Applying them locally in the inhomogeneous mean flows requires the local diffusivity value to be determined by the local mean-state properties, and to what extent this approximation holds also remains a nontrivial problem (e.g., Pavan and Held 1996; Chang and Held 2019). Therefore, a better understanding of these questions seems necessary for developing EBM theories with spatially varying and climate-state-dependent diffusivities.

Last, it is worth comparing our diffusive EBM theories with the common approach to diagnosing polar versus tropical temperature change "contributions" from terms in the local energy budgets (e.g., Winton 2006; Crook et al. 2011; Feldl and Roe 2013; Pithan and Mauritsen 2014). Recall that in our theories, the key parameter μ characterizes the relative roles of radiative restoring versus advective (as encapsulated by meridional diffusion) restoring of forcing. So long as μ stays finite, that is, $\mathcal{D} \neq 0$ and $B \nrightarrow \infty$, we expect any local forcing to not be entirely radiatively restored at the same latitude and will invoke diffusive energy transport across latitudes. This nonlocal nature of transport means that the temperatures at different latitudes interact. It is then impossible to independently study the changes in local temperature and local energy budget in one region assuming the others are held fixed. Therefore, while both approaches try to understand the polar amplification based on the top-of-atmosphere energy balance, they are fundamentally different in how they conceptualize the relationship between the local temperature response and forcing (Merlis 2014).

6. Conclusions

There have been many recent applications of moist EBMs to climate change research questions. These have started from emulating poleward energy transport (Frierson et al. 2007; Hwang and Frierson 2010; Hwang et al. 2011) and subsequently centered on the pattern of warming (Bonan et al. 2018; Armour et al. 2019; Feldl and Merlis 2021; Beer and Eisenman 2022; Hill et al. 2022) and hydrological cycle (Siler et al. 2018; Bonan et al. 2023). The typical assumption is that, to leading order, both the spatial structure of the climatological diffusivity and its changes with warming are negligible. This ansatz seems to persist largely because it gives a reasonable agreement between EBM solutions and GCM simulations rather than there being solid justifications for the assumption. In parallel, there is a large body of literature on theories of atmospheric diffusivities (e.g., Green 1970; Stone 1972; Held and Larichev 1996; Barry et al. 2002; Chang and Held 2021; Gallet and Ferrari 2021; Chang and Held 2022) and diagnosed diffusivity changes in GCM simulations (e.g., Frierson et al. 2007; Bischoff and Schneider 2014; Liu et al. 2017; Merlis et al. 2022; Lu et al. 2022). This suggests the need to directly assess the possible role that diffusivity changes play in EBM solutions of climate change.

Here, we extend the analytic EBM theory for the large-scale temperature gradient developed in Merlis and Henry (2018) to include climate-state dependence of globally uniform diffusivities. As we are focused on the pattern of warming, the theory was developed for diffusivities that depend on the global-mean temperature T_0 and the large-scale temperature and MSE contrasts encapsulated via their second-order Legendre polynomial components, T_2 and h_2, respectively. For both diffusivity formulations, the sensitivities of T_2 and h_2 to T_0 are found to depend on two key parameters: μ [Eq. (22)] and χ [Eq. (23)]. The former measures the relative role of radiative versus diffusive damping on imposed energy

flux anomalies, which is introduced as an intrinsic parameter describing the local energy balance in EBMs. The latter measures the nonlinear temperature dependence and the origin of T_0 dependence due to the presence of moisture, which is itself constrained by CC sensitivity and the ratio of the climatological latent to total energy gradient. The theory for the warming pattern obtained from the analytic expressions compares well to numerical EBM solutions.

For the global-mean temperature-dependent diffusivity $\mathcal{D} = \mathcal{D}(T_0) \propto \gamma T_0$, two critical values for the prescribed diffusivity sensitivity $\gamma = \partial_{T_0} \ln \mathcal{D}$ are identified: $\gamma = \gamma_{c,T} = -\chi < 0$ [$\approx -3\%$ K^{-1}; Eq. (13)] for uniform temperature increase and $\gamma = \gamma_{c,h} = \mu\chi > 0$ [$\approx 1.5\%$ K^{-1}; Eq. (17)] for uniform MSE increase. Each has corresponded to a baseline calculation for the warming response. The uniform temperature increase was argued by Shaw and Voigt (2016) to be a natural starting point to estimate the diffusivity response to warming. Accordingly, they derived the diffusivity dependence on global mean temperature that is regulated by CC sensitivity, which is recovered by $\gamma_{c,T}$ in our theory. The uniform MSE increase was argued by Byrne and O'Gorman (2013) as an alternative starting point for the pattern of surface warming, although they were focused on tropical land–sea contrasts in warming rather than the equator-to-pole contrast. Merlis and Henry (2018) found that it does not satisfy energy balance with constant diffusivity, and we now show that it can be a EBM solution with a diffusivity increasing with T_0 at the rate of $\gamma_{c,h}$.

For the diffusivity that depends on temperature and MSE contrasts $\mathcal{D} = \mathcal{D}(T_2, h_2) \propto T_2^n h_2^m$ and $n \geq 0$, $m \geq 0$, the temperature gradient is always found to reduce and the MSE gradient is always found to enhance when T_0 is increased. We acknowledge that there remains an incomplete understanding of the diffusivity change with global warming, and more generally, a diffusivity theory that is well justified for Earth's atmosphere. However, to the extent that the general form of diffusivity considered here can capture the essence of the previously proposed theories (Held and Larichev 1996; Barry et al. 2002; Frierson et al. 2007; Chang and Held 2022; Lu et al. 2022), it is perhaps fair to expect that a changing diffusivity only modulates the amplitude but does not eliminate the polar amplification in warm climates. Relatedly, the equator-to-pole MSE contrast is always amplified, since the effect of temperature dependence of saturation specific humidity wins over the effect of temperature gradient change. Therefore, the two limiting cases of uniform temperature or MSE increase discussed in $\mathcal{D}(T_0)$ theory indeed turn out to be relevant benchmarks in thinking about the role of diffusivity changes on the pattern of warming.

Due to the opposite change of temperature and MSE gradients, the diffusivity sensitivity [internally determined by $\mathcal{D}(T_2, h_2)$] is consistently found to be bounded by $\gamma_{c,T} < \gamma < \gamma_{c,h}$. The compensating effect of the two gradients that limits the diffusivity change was speculated by Chang and Held (2022) as an explanation for the stiffness of the diffusivity in response to radiative forcing (Held 2007). The analytic theory here provides an explicit quantitative means of evaluating this speculation. Likewise, the theory also offers a quantitative expression for a similar argument of Lu et al. (2022). Assuming a temperature gradient dependence, they argued that the diffusivity has to decrease but can only decrease moderately with warming, which they confirmed in both EBM and GCM numerical results. In our analytic theory, this is equivalent to setting $m = 0$, which gives $\gamma_{c,T} < \gamma < 0$ and further limits the diffusivity sensitivity.

That the diffusivity change with warming is limited due to dynamical constraints likely explains why the constant-diffusivity EBM in Merlis and Henry (2018) can already provide a decent estimate for polar amplification. In addition, it offers a physical reasoning for why a model- and climate-invariant diffusivity has empirically been successful in some previous EBM studies when emulating comprehensive GCM simulations (e.g., Hwang and Frierson 2010; Bonan et al. 2018; Armour et al. 2019). Perhaps less appreciated, it is with the adequacy of constant diffusivity approximation that these studies can simply attribute the different patterns of warming to the different patterns of climate feedbacks and their associated physical processes without explicitly concerning the change of atmospheric circulation. In fact, these studies focus on the intermodel spread of the simulated Arctic warming, which is attributed to the spread of localized Arctic feedbacks (e.g., Hwang et al. 2011; Roe et al. 2015; Bonan et al. 2018). Mechanisms for such a localized phenomenon may be distinguished from the ones for the change in planetary-scale meridional temperature gradient discussed here, which is governed by the change in planetary-scale poleward energy transport. For this reason, the choice of the control diffusivity value, its changes with warming, or its spatial structure in EBMs, are likely to play an even more diminished role in their specific metric of polar amplification.

Finally, we emphasize that the diffusivity forms $\mathcal{D}(T_0)$ and $\mathcal{D}(T_2, h_2)$ studied here are motivated by and in hopes of making connection to previous studies. However, they are also arguably the only two relevant forms that offer feasible analytic solutions with our current EBM formulations. To ensure we obtain a diffusivity closure suitable for analytic EBM theories, we inevitably have to ignore other factors that are potentially important in determining the diffusivity response to warming, especially the role of vertical thermal structure (e.g., Lapeyre and Held 2004; O'Gorman 2011; Chang and Held 2022; Brown et al. 2023). Additional research to arrive at formulations for the diffusivity of moist atmospheric macroturbulence in terms of the surface variables that govern EBMs or formulations for EBMs that incorporate vertical information would help further extend the theory presented here. As a reminder, our analytic and numerical EBM solutions assume spatially uniform forcing, feedbacks, and diffusivity. There is also no seasonal cycle in the insolation and co-albedo to represent the time evolution of clouds and sea ice (e.g., Feldl and Merlis 2021). More fundamentally, our OLR formulation is subject to the known limitations of the top-of-atmosphere feedback framework when applied to the polar regions (e.g., Payne et al. 2015; Cronin and Jansen 2016; Henry and Merlis 2020; Henry et al. 2021). Relaxing these assumptions individually will help bridge the remaining gap between EBM theory and temperature change in GCM simulations.

Acknowledgments. We thank Harry Llewellyn for performing an early version of the numerical calculations with

global-mean temperature-dependent diffusivity. We thank Nicole Feldl for encouraging this research, Isaac Held, Pablo Zurita-Gotor, and Yen-Ting Hwang for helpful discussions, and three anonymous reviewers for their feedback. We are grateful for the support of the Cooperative Institute for Modelling Earth Systems under Award NA18OAR4320123 from the National Oceanic and Atmospheric Administration, U.S. Department of Commerce.

Data availability statement. The code to reproduce the numerical EBM calculations and figures is available at https://github.com/cyinchang/EBM-diffusivity.

APPENDIX

We here express the sensitivities of T_2, h_2, and $\mathcal{D}$ as functions of μ [Eq. (22)] and χ [Eq. (23)] for different diffusivity formulations. For $\mathcal{D} = \overline{\mathcal{D}}$, Eqs. (7) and (10) can be rewritten as

$$\left.\frac{\partial \ln T_2}{\partial T_0}\right|_{\overline{T}} = \frac{-\chi}{1+\mu} \tag{A1}$$

and

$$\left.\frac{\partial \ln h_2}{\partial T_0}\right|_{\overline{T}} = \frac{\chi\mu}{1+\mu}. \tag{A2}$$

For $\mathcal{D} = \mathcal{D}(T_0)$ [Eq. (2)], Eqs. (12) and (16) can be rewritten as

$$\left.\frac{\partial \ln T_2}{\partial T_0}\right|_{\overline{T}} = \frac{-(\chi+\gamma)}{1+\mu} \tag{A3}$$

and

$$\left.\frac{\partial \ln h_2}{\partial T_0}\right|_{\overline{T}} = \frac{(\chi\mu-\gamma)}{1+\mu}. \tag{A4}$$

For $\mathcal{D} = \mathcal{D}(T_2, h_2)$ [Eq. (3)], Eqs. (19), (20) and (21) can be rewritten respectivley as

$$\left.\frac{\partial \ln T_2}{\partial T_0}\right|_{\overline{T}} = \frac{-\chi(m+1)}{m+n+1+\mu}, \tag{A5}$$

$$\left.\frac{\partial \ln h_2}{\partial T_0}\right|_{\overline{T}} = \frac{\chi(\mu+n)}{m+n+1+\mu}, \tag{A6}$$

and

$$\left.\frac{\partial \ln \mathcal{D}}{\partial T_0}\right|_{\overline{T}} = \frac{\chi(\mu m-n)}{m+n+1+\mu}. \tag{A7}$$

REFERENCES

Armour, K. C., N. Siler, A. Donohoe, and G. H. Roe, 2019: Meridional atmospheric heat transport constrained by energetics and mediated by large-scale diffusion. *J. Climate*, **32**, 3655–3680, https://doi.org/10.1175/JCLI-D-18-0563.1.

Barry, L., G. C. Craig, and J. Thuburn, 2002: Poleward heat transport by the atmospheric heat engine. *Nature*, **415**, 774–777, https://doi.org/10.1038/415774a.

Beer, E., and I. Eisenman, 2022: Revisiting the role of the water vapor and lapse rate feedbacks in the Arctic amplification of climate change. *J. Climate*, **35**, 2975–2988, https://doi.org/10.1175/JCLI-D-21-0814.1.

Bischoff, T., and T. Schneider, 2014: Energetic constraints on the position of the intertropical convergence zone. *J. Climate*, **27**, 4937–4951, https://doi.org/10.1175/JCLI-D-13-00650.1.

Bonan, D. B., K. C. Armour, G. H. Roe, N. Siler, and N. Feldl, 2018: Sources of uncertainty in the meridional pattern of climate change. *Geophys. Res. Lett.*, **45**, 9131–9140, https://doi.org/10.1029/2018GL079429.

——, N. Siler, G. H. Roe, and K. C. Armour, 2023: Energetic constraints on the pattern of changes to the hydrological cycle under global warming. *J. Climate*, **36**, 3499–3522, https://doi.org/10.1175/JCLI-D-22-0337.1.

Brown, M. L., O. Pauluis, and E. P. Gerber, 2023: Scaling for saturated moist quasigeostrophic turbulence. *J. Atmos. Sci.*, **80**, 1481–1498, https://doi.org/10.1175/JAS-D-22-0215.1.

Byrne, M. P., and P. A. O'Gorman, 2013: Land–ocean warming contrast over a wide range of climates: Convective quasi-equilibrium theory and idealized simulations. *J. Climate*, **26**, 4000–4016, https://doi.org/10.1175/JCLI-D-12-00262.1.

Chang, C.-Y., and I. M. Held, 2019: The control of surface friction on the scales of baroclinic eddies in a homogeneous quasigeostrophic two-layer model. *J. Atmos. Sci.*, **76**, 1627–1643, https://doi.org/10.1175/JAS-D-18-0333.1.

——, and ——, 2021: The parameter dependence of eddy heat flux in a homogeneous quasigeostrophic two-layer model on a β plane with quadratic friction. *J. Atmos. Sci.*, **78**, 97–106, https://doi.org/10.1175/JAS-D-20-0145.1.

——, and ——, 2022: A scaling theory for the diffusivity of poleward eddy heat transport based on Rhines scaling and the global entropy budget. *J. Atmos. Sci.*, **79**, 1743–1758, https://doi.org/10.1175/JAS-D-21-0242.1.

Cronin, T. W., and M. F. Jansen, 2016: Analytic radiative-advective equilibrium as a model for high-latitude climate. *Geophys. Res. Lett.*, **43**, 449–457, https://doi.org/10.1002/2015GL067172.

Crook, J. A., P. M. Forster, and N. Stuber, 2011: Spatial patterns of modeled climate feedback and contributions to temperature response and polar amplification. *J. Climate*, **24**, 3575–3592, https://doi.org/10.1175/2011JCLI3863.1.

Feldl, N., and G. H. Roe, 2013: The nonlinear and nonlocal nature of climate feedbacks. *J. Climate*, **26**, 8289–8304, https://doi.org/10.1175/JCLI-D-12-00631.1.

——, and T. M. Merlis, 2021: Polar amplification in idealized climates: The role of ice, moisture, and seasons. *Geophys. Res. Lett.*, **48**, e2021GL094130, https://doi.org/10.1029/2021GL094130.

Flannery, B. P., 1984: Energy balance models incorporating transport of thermal and latent energy. *J. Atmos. Sci.*, **41**, 414–421, https://doi.org/10.1175/1520-0469(1984)041<0414:EBMITO>2.0.CO;2.

Frierson, D. M. W., I. M. Held, and P. Zurita-Gotor, 2007: A gray-radiation aquaplanet moist GCM. Part II: Energy transports in altered climates. *J. Atmos. Sci.*, **64**, 1680–1693, https://doi.org/10.1175/JAS3913.1.

Gallet, B., and R. Ferrari, 2021: A quantitative scaling theory for meridional heat transport in planetary atmospheres and oceans. *AGU Adv.*, **2**, e2020AV000362, https://doi.org/10.1029/2020AV000362.

Green, J. S. A., 1970: Transfer properties of the large-scale eddies and the general circulation of the atmosphere. *Quart. J. Roy. Meteor. Soc.*, **96**, 157–185, https://doi.org/10.1002/qj.49709640802.

Held, I. M., 1999: The macroturbulence of the troposphere. *Tellus*, **51A**, 59–70, https://doi.org/10.3402/tellusa.v51i1.12306.

——, 2007: Progress and problems in large-scale atmospheric dynamics. *The Global Circulation of the Atmosphere*, T. Schneider and A. H. Sobel, Eds., Princeton University Press, 1–21.

——, and V. D. Larichev, 1996: A scaling theory for horizontally homogeneous, baroclinically unstable flow on a beta plane. *J. Atmos. Sci.*, **53**, 946–952, https://doi.org/10.1175/1520-0469(1996)053<0946:ASTFHH>2.0.CO;2.

Henry, M., and T. M. Merlis, 2020: Forcing dependence of atmospheric lapse rate changes dominates residual polar warming in solar radiation management climate scenarios. *Geophys. Res. Lett.*, **47**, e2020GL087929, https://doi.org/10.1029/2020GL087929.

——, ——, N. J. Lutsko, and B. E. J. Rose, 2021: Decomposing the drivers of polar amplification with a single-column model. *J. Climate*, **34**, 2355–2365, https://doi.org/10.1175/JCLI-D-20-0178.1.

Hill, S. A., N. J. Burls, A. Fedorov, and T. M. Merlis, 2022: Symmetric and antisymmetric components of polar-amplified warming. *J. Climate*, **35**, 3157–3172, https://doi.org/10.1175/JCLI-D-20-0972.1.

Hwang, Y.-T., and D. M. W. Frierson, 2010: Increasing atmospheric poleward energy transport with global warming. *Geophys. Res. Lett.*, **37**, L24807, https://doi.org/10.1029/2010GL045440.

——, ——, and J. E. Kay, 2011: Coupling between Arctic feedbacks and changes in poleward energy transport. *Geophys. Res. Lett.*, **38**, L17704, https://doi.org/10.1029/2011GL048546.

Kim, D., S. M. Kang, Y. Shin, and N. Feldl, 2018: Sensitivity of polar amplification to varying insolation conditions. *J. Climate*, **31**, 4933–4947, https://doi.org/10.1175/JCLI-D-17-0627.1.

Lapeyre, G., and I. M. Held, 2004: The role of moisture in the dynamics and energetics of turbulent baroclinic eddies. *J. Atmos. Sci.*, **61**, 1693–1710, https://doi.org/10.1175/1520-0469(2004)061<1693:TROMIT>2.0.CO;2.

Lindzen, R. S., and B. Farrell, 1980: The role of polar regions in global climate, and a new parameterization of global heat transport. *Mon. Wea. Rev.*, **108**, 2064–2079, https://doi.org/10.1175/1520-0493(1980)108<2064:TROPRI>2.0.CO;2.

Liu, X., D. S. Battisti, and G. H. Roe, 2017: The effect of cloud cover on the meridional heat transport: Lessons from variable rotation experiments. *J. Climate*, **30**, 7465–7479, https://doi.org/10.1175/JCLI-D-16-0745.1.

Lu, J., W. Zhou, H. Kong, L. R. Leung, B. Harrop, and F. Song, 2022: On the diffusivity of moist static energy and implications for the polar amplification response to climate warming. *J. Climate*, **35**, 7127–7146, https://doi.org/10.1175/JCLI-D-21-0721.1.

Mbengue, C., and T. Schneider, 2018: Linking Hadley circulation and storm tracks in a conceptual model of the atmospheric energy balance. *J. Atmos. Sci.*, **75**, 841–856, https://doi.org/10.1175/JAS-D-17-0098.1.

Merlis, T. M., 2014: Interacting components of the top-of-atmosphere energy balance affect changes in regional surface temperature. *Geophys. Res. Lett.*, **41**, 7291–7297, https://doi.org/10.1002/2014GL061700.

——, and M. Henry, 2018: Simple estimates of polar amplification in moist diffusive energy balance models. *J. Climate*, **31**, 5811–5824, https://doi.org/10.1175/JCLI-D-17-0578.1.

——, N. Feldl, and R. Caballero, 2022: Changes in poleward atmospheric energy transport over a wide range of climates: Energetic and diffusive perspectives and a priori theories. *J. Climate*, **35**, 6533–6548, https://doi.org/10.1175/JCLI-D-21-0682.1.

Mooring, T. A., and T. A. Shaw, 2020: Atmospheric diffusivity: A new energetic framework for understanding the midlatitude circulation response to climate change. *J. Geophys. Res. Atmos.*, **125**, e2019JD031206, https://doi.org/10.1029/2019JD031206.

North, G. R., 1975: Theory of energy-balance climate models. *J. Atmos. Sci.*, **32**, 2033–2043, https://doi.org/10.1175/1520-0469(1975)032<2033:TOEBCM>2.0.CO;2.

——, R. F. Cahalan, and J. A. Coakley Jr., 1981: Energy balance climate models. *Rev. Geophys.*, **19**, 91–121, https://doi.org/10.1029/RG019i001p00091.

O'Gorman, P. A., 2011: The effective static stability experienced by eddies in a moist atmosphere. *J. Atmos. Sci.*, **68**, 75–90, https://doi.org/10.1175/2010JAS3537.1.

——, and T. Schneider, 2008: Energy of midlatitude transient eddies in idealized simulations of changed climates. *J. Climate*, **21**, 5797–5806, https://doi.org/10.1175/2008JCLI2099.1.

Pavan, V., and I. M. Held, 1996: The diffusive approximation for eddy fluxes in baroclinically unstable jets. *J. Atmos. Sci.*, **53**, 1262–1272, https://doi.org/10.1175/1520-0469(1996)053<1262:TDAFEF>2.0.CO;2.

Payne, A. E., M. F. Jansen, and T. W. Cronin, 2015: Conceptual model analysis of the influence of temperature feedbacks on polar amplification. *Geophys. Res. Lett.*, **42**, 9561–9570, https://doi.org/10.1002/2015GL065889.

Pithan, F., and T. Mauritsen, 2014: Arctic amplification dominated by temperature feedbacks in contemporary climate models. *Nat. Geosci.*, **7**, 181–184, https://doi.org/10.1038/ngeo2071.

Roe, G. H., N. Feldl, K. C. Armour, Y.-T. Hwang, and D. M. W. Frierson, 2015: The remote impacts of climate feedbacks on regional climate predictability. *Nat. Geosci.*, **8**, 135–139, https://doi.org/10.1038/ngeo2346.

Russotto, R. D., and M. Biasutti, 2020: Polar amplification as an inherent response of a circulating atmosphere: Results from the TRACMIP aquaplanets. *Geophys. Res. Lett.*, **47**, e2019GL086771, https://doi.org/10.1029/2019GL086771.

Schneider, T., 2006: The general circulation of the atmosphere. *Annu. Rev. Earth Planet. Sci.*, **34**, 655–688, https://doi.org/10.1146/annurev.earth.34.031405.125144.

Shaw, T. A., and A. Voigt, 2016: What can moist thermodynamics tell us about circulation shifts in response to uniform warming? *Geophys. Res. Lett.*, **43**, 4566–4575, https://doi.org/10.1002/2016GL068712.

Siler, N., G. H. Roe, and K. C. Armour, 2018: Insights into the zonal-mean response of the hydrologic cycle to global warming from a diffusive energy balance model. *J. Climate*, **31**, 7481–7493, https://doi.org/10.1175/JCLI-D-18-0081.1.

Stone, P. H., 1972: A simplified radiative-dynamical model for the static stability of rotating atmospheres. *J. Atmos. Sci.*, **29**, 405–418, https://doi.org/10.1175/1520-0469(1972)029<0405:ASRDMF>2.0.CO;2.

Winton, M., 2006: Amplified Arctic climate change: What does surface albedo feedback have to do with it? *Geophys. Res. Lett.*, **33**, L03701, https://doi.org/10.1029/2005GL025244.

Wu, Y., M. Ting, R. Seager, H.-P. Huang, and M. A. Cane, 2011: Changes in storm tracks and energy transports in a warmer climate simulated by the GFDL CM2.1 model. *Climate Dyn.*, **37**, 53–72, https://doi.org/10.1007/s00382-010-0776-4.